A Sensory Soft Robotic Gripper Capable of Learning-Based Object Recognition and Force-Controlled Grasping

Zhanfeng Zhou, Runze Zuo, Binbin Ying, Junhui Zhu, Yong Wang, Xin Wang, *Member, IEEE*, and Xinyu Liu, *Member, IEEE*

***Abstract*— Soft robotic grippers possess high structural compliance and adaptability, allowing them to grasp objects with unknown and irregular shapes and sizes. To enable more dexterous manipulation, soft sensors that are similar in mechanical properties to common elastomer materials are desired to be integrated into soft grippers. In this paper, we develop ionic hydrogel-based strain and tactile sensors and integrate these sensors into a three-finger soft gripper for learning-based object recognition and force-controlled grasping. Such hydrogel-based sensors have excellent conductivity, high stretchability and toughness, good ambient stability, and unique antifreezing property; they can be readily attached to a soft gripper at desired locations for strain and tactile sensing. By using a deep-learning model, the sensory soft gripper is demonstrated to be capable of grasping and recognizing objects at both room and freezing temperatures, and achieving close to 100% recognition accuracy for ten typical objects. Moreover, the capacitive tactile feedback of the gripper is utilized to develop a closed-loop force controller and realize force-controlled grasping of fragile or highly deformable objects. A new slip detection and compensation strategy is also proposed and validated for the sensory gripper for adjusting the grasping force in real time upon detecting slippage.**

***Note to Practitioners*—The multimodal sensation of a soft robotic gripper could enrich its grasping functionalities and improve its manipulation performance. This research integrates novel antifreezing ionic hydrogel-based strain and tactile sensors into a three-finger soft robotic gripper for learning-based object recognition and force-controlled grasping. Constructed from a highly stretchable, ambient-stable, and antifreezing ionic hydrogel, the strain and tactile sensors can be readily integrated at the desired locations on the soft gripper, and can reliably operate at both ambient and freezing temperatures with excellent mechanical and electrical properties. Based on the feedback of the strain and tactile sensors, a deep learning model is employed to enable high-accuracy object recognition while grasping, which can be useful for manipulation in vision-free environments. Closed-loop force control and slip compensation strategies are also demonstrated for reliably grasping fragile/deformable objects and handling slip events during the manipulation of heavy objects. The sensory soft gripper and the associated object recognition and force control methods could find practical applications in a variety of robotic manipulation tasks.**

***Index Terms*—Sensory soft gripper, hydrogel-based sensor, object recognition, force-controlled grasp, slip detection and compensation.**

Manuscript received 18 March 2022; revised 13 August 2022; accepted 30 October 2022. This article was recommended for publication by Associate Editor T. Xu and Editor L. Zhang upon evaluation of the reviewers' comments. This work was supported in part by the Natural Sciences and Engineering Research Council of Canada under Grant RGPIN-2017-06374 and Grant RGPAS-2017-507980, in part by the Canada Foundation for Innovation under Grant JELF-37812, in part by the University of Toronto (CARTE Seed Fund), and in part by the Mitacs Canada (Summer Research Scholarship to R.Z.). *(Zhanfeng Zhou and Runze Zuo contributed equally to this work.) (Corresponding author: Xinyu Liu.)*

Zhanfeng Zhou, Runze Zuo, and Xinyu Liu are with the Department of Mechanical and Industrial Engineering, University of Toronto, Toronto, ON M5S 3G8, Canada (e-mail: xyliu@mie.utoronto.ca).

Binbin Ying is with the Department of Mechanical Engineering, Massachusetts Institute of Technology, Cambridge, MA 02139 USA.

Junhui Zhu and Yong Wang are with the School of Electronic and Information Engineering, Suzhou University of Science and Technology, Suzhou 215009, China.

Xin Wang is with the Department of Mechanical and Aerospace Engineering, Jilin University, Changchun 130012, China.

This article has supplementary material provided by the authors and color versions of one or more figures available at https://doi.org/10.1109/TASE.2022.3228255.

Digital Object Identifier 10.1109/TASE.2022.3228255

I. Introduction

SOFT robots possess several attractive advantages over traditional rigid robots, including high structural compliance, excellent morphological adaptability, and high safety level for interactions with humans and their environment [1], [2], [3], [4]. Their flexible and compliant structures allow the soft robots to readily adapt to environmental uncertainties and unpredictable object shapes, making them particularly suitable for various applications, including delicate grasping [5], [6], dexterous manipulation [7], and human-robot interaction and collaboration [8]. Traditional rigid robotic grippers and manipulators are capable of performing sophisticated grasping tasks in structured environments based on accurate modeling, as well as precise feedback control of the robotic manipulation system [9], [10]. However, they lack the adaptability to uncertainties in unstructured environments. In contrast, soft robotic hands and grippers provide the opportunity to grasp objects of unknown and irregular shapes and sizes [11].

Apart from the structural compliance that enhances the adaptability of a soft gripper, strain and tactile sensing could further improve its manipulation performance and enable new functionalities, including tactile object recognition and closed-loop position/force control. There have been several types of soft sensor designs proposed for strain and tactile sensing on soft grippers. A popular design is based on conductive elastomer composites such as carbon nanotube-doped PDMS [12] and laser-induced graphene [13]. Integrating such conductive

sensing materials into an elastomer material increases the stiffness or structural compliance of the sensing material and thus causes a large compliance mismatch between the sensor layer and the gripper structure. Another type of soft sensors is liquid metal-based sensors [14], [15], [16], which employ conductive liquid metals filled in elastomer microchannels as a resistive sensing component. These liquid metal-embedded elastomers can be used to detect multi-axis strains [14], contact pressures [15], and normal and in-plane shear forces [16]. However, the microchannel fabrication involves soft lithography, which requires a certain level of skills and a certain type of facility for microfabrication that is not readily accessible by roboticists. Embedded optical sensors in elastomer structures represent another popular option. Examples include optical fiber-based sensors integrated into robotic end-effectors for the measurement of contact force [17], optical waveguide sensors that measure strain, pressure, and curvature [18], [19], and vision-based tactile sensors incorporated into gripper fingers for proprioceptive and tactile sensing (by visually tracking contact-induced deformations of the gripper finger) [20]. However, these optical sensors usually require the integration of light sources and optical detectors within soft grippers, resulting in a more complex gripper design. In addition, integrating rigid light sources and optical detectors may reduce the compliance of soft grippers.

Moreover, a novel bladder-based soft air pressure sensor was developed [6] and integrated into the Magic Ball origami gripper [21]. This new kind of soft bladder sensor is easy to fabricate and integrate with a soft body. However, the soft bladder sensor can only be used on specific origami grippers by carefully selecting the placement of sensors. Integrating commercial flex bend sensors and force sensors into the constraint layer of soft grippers is also a popular sensing approach. Homberg et al. [3], [22] integrated commercial flex bend sensors into the constraint layer and commercial force sensors at the tip of the soft fingers to realize finger-controlled grasping and object identification. She et al. [23] also embedded a commercial flexure sensor in the center line of the shape memory alloy (SMA) actuated finger body to provide feedback on finger shape for precise finger position control. However, the integration of the commercial flex bend sensor will greatly affect the compliance of the soft fingers. Therefore, the development of new soft/stretchable sensors and facile integration strategies are still highly desired.

In the field of stretchable conductive materials, carbon nanotubes [12], [24], carbon black [25], ionic fluids [26], ionogels (organic ion liquid filled with fumed silica nanoparticles) [27], and ionic hydrogels [28], [29], [30] have been demonstrated to be effective in strain and pressure sensing for soft robotics. Among these materials, ionic hydrogels possess several unique properties, which make them suitable for wearable and stretchable sensing, including excellent conductivity, high stretchability, and reasonable biocompatibility. Nevertheless, they still have several limitations. For example, pristine ionic hydrogels lack ambient stability when exposed to harsh environments (e.g., hot or freezing environments), due to the evaporation or freezing of their water content. This impedes their practical use on soft grippers for applications such as frozen food sorting and packaging. In addition, the poor surface adhesion of ionic hydrogels to the soft robotic bodies during large deformation also raises technical challenges when integrating sensors into the soft robotic system. A facile "stick-on" method based on a silane chemistry mechanism was proposed to achieve strong adhesion between hydrogels and elastomers and thus enabled a hydrogel-based large-strain sensor to be integrated on soft robots [31]. However, such bonding method need a long-time heating process, which makes the sensor integration time-consuming and complicated. We recently developed an ambient-stable and antifreezing ionic hydrogel that can adhere to most elastomer surfaces strongly and quickly, which is promising for use on soft robots for a range of application scenarios [32].

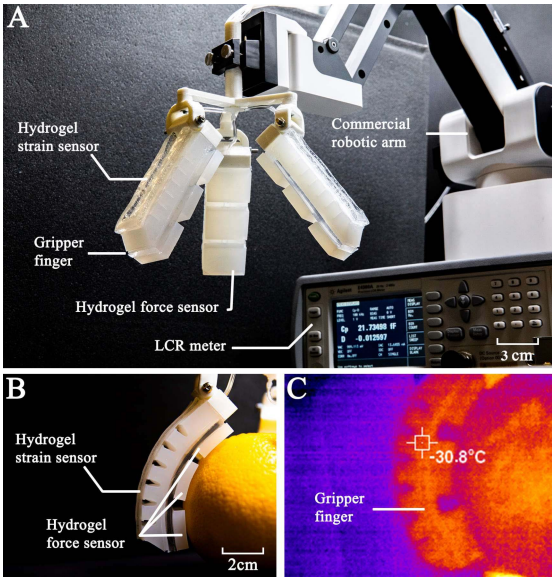

Fig. 1. Soft gripper with the capability of object recognition and force-controlled grasping. (A) Soft gripper with nine hydrogel-based force sensors and three hydrogel-based strain sensors, connected to a robotic arm for object manipulation, and an LCR meter for sensor readout acquisition. (B) The three fingers have the ability to recognize objects (such as orange) during grasping. (C) The gripper and its hydrogel-based sensors can work in extremely cold temperatures.

Based on the antifreezing ionic hydrogel, this paper presents a new sensory three-finger soft gripper with hydrogel-based stretchable strain and tactile sensors (Fig. 1). The ionic hydrogel utilizes a double-network design and contains inorganic ions and a hygroscopic/cryoprotective substance to make it conductive, antifreezing, and ambient-stable. A resistive strain sensor, based on the strain-induced resistance change of the ionic hydrogel, is attached to the back surface of each gripper finger to measure the finger bending angle. Three capacitive tactile sensors, constructed from two ionic hydrogel layers sandwiching a dielectric elastomer layer, are integrated on the inner surface of each finger for tactile sensing. The strain and tactile sensors can operate at both room and freezing temperatures. With the feedback of the strain and tactile sensors, a deep-learning model is employed to realize object recognition both at room and freezing temperatures, and a closed-loop force controller is designed to allow force-controlled grasp and slip detection and compensation.

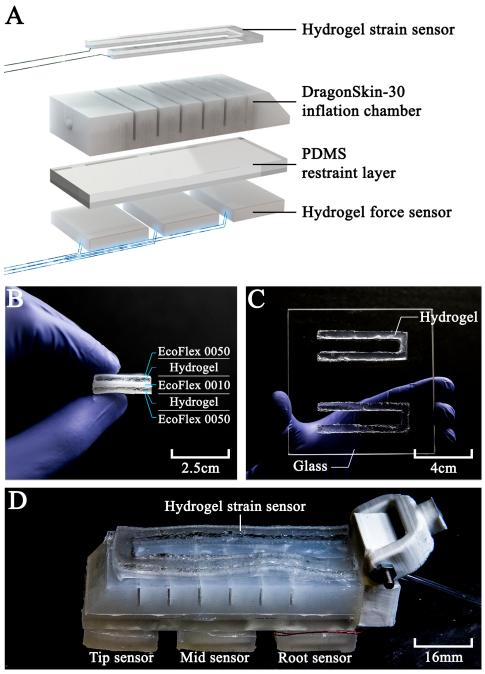

Fig. 2. Design of the sensory soft gripper. (A) The schematic of the gripper design. (B) A multi-layer capacitive tactile sensor. (C) A resistive strain sensor on a glass substrate. (D) A soft gripper finger integrated with three tactile sensors and one strain sensor.

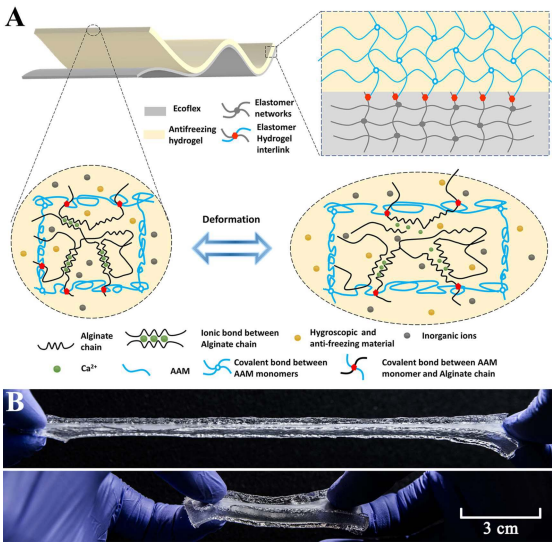

Fig. 3. Design of the antifreezing ionic hydrogel. (A) Schematic illustration of the ionic hydrogel design and its tough interfacial bonding with EcoFlex through a covalently anchored hydrogel polymer network on the EcoFlex surface. (B) Demonstration of the stretchability of the hydrogel-based resistive sensor.

This article is an extended version of a previous conference paper [33]. In this journal version, we include a new closed-loop force controller for the sensory soft gripper and propose a slip detection and compensation strategy based on the tactile sensor feedback. More experiments were conducted on the force-controlled grasping of fragile or highly deformable objects and automated slip detection and compensation during object grasping. In addition, more object recognition experiments have been conducted on objects with different orientations to further demonstrate the effectiveness of the deep learning model. Finally, more technical details and discussions have been added.

II. Sensory Soft Gripper Design and Fabrication

A. Soft Gripper Design and Fabrication

The soft gripper (Fig. 1A) consists of three pneumatically actuated soft fingers mounted on a rigid 3D-printed palm base. The design of the soft fingers is based on the pneumatic network design previously reported in [34] and [35]. As shown in Fig. 2A, each soft finger is comprised of a flexible silicone layer (Dragon Skin 30) molded with interconnected parallel chambers and a constraint layer (polydimethylsiloxane or PDMS). The bonding of the two layers forms an internal pneumatic network that bends the soft finger towards the constraint layer side under inflation. The lost-wax casting process [36] was used to fabricate the soft fingers. A strain sensor is integrated on the back surface of each soft finger, and three tactile sensors on its inner surface. All of these sensors are constructed from the antifreezing ionic hydrogel (see Video S1, Supplementary Video). The net weight of the soft pneumatic gripper without the valves and the power source is 255 g, and the maximum grasping payload is 600 g (more than 2 times the gripper's weight). The sensor design, fabrication, and integration with the soft fingers (Video S1, Supplementary Videos) will be described in detail in the following sections.

B. Ionic Hydrogel Synthesis

The antifreezing ionic hydrogel is comprised of a touch double-network matrix of hybrid cross-linked and interpenetrating alginate-polyacrylamide (Alg-PAAm) doped with inorganic ions (Na^+ and Cl^-) and a hygroscopic/cryoprotective substance, glycerol (Fig. 3A). The Alg and PAAm were selected for the construction of the hydrogel matrix due to their outstanding mechanical properties that enable them to efficiently dissipate energy under deformation [37]. To reduce the loss of water and lower the ice crystallization temperature of the hydrogel, glycerol was incorporated into the tough hydrogel matrix as a hygroscopic and cryoprotective material. The ionic hydrogel has been experimentally demonstrated to be antifreezing (glass transition temperature: -95 °C), highly ambient-stable (with negligible mass loss after 30 days of storage), and highly stretchable (it can sustain up to 1975% strain without rupture) [32]. To form a strong bond between the ionic hydrogel and EcoFlex, an *in-situ* chemical grafting process was used to graft methacrylate groups on the surface of the chemisorbed Ecoflex to the PAAm network during curing [38]. This tough bonding can further enhance the ambient stability of the ionic hydrogel and is also crucial to develop durable strain and tactile sensors with high signal fidelity.

C. Capacitive Tactile Sensor

The capacitive tactile sensor consists of two ionic hydrogel layers sandwiching a dielectric layer (EcoFlex-0010),

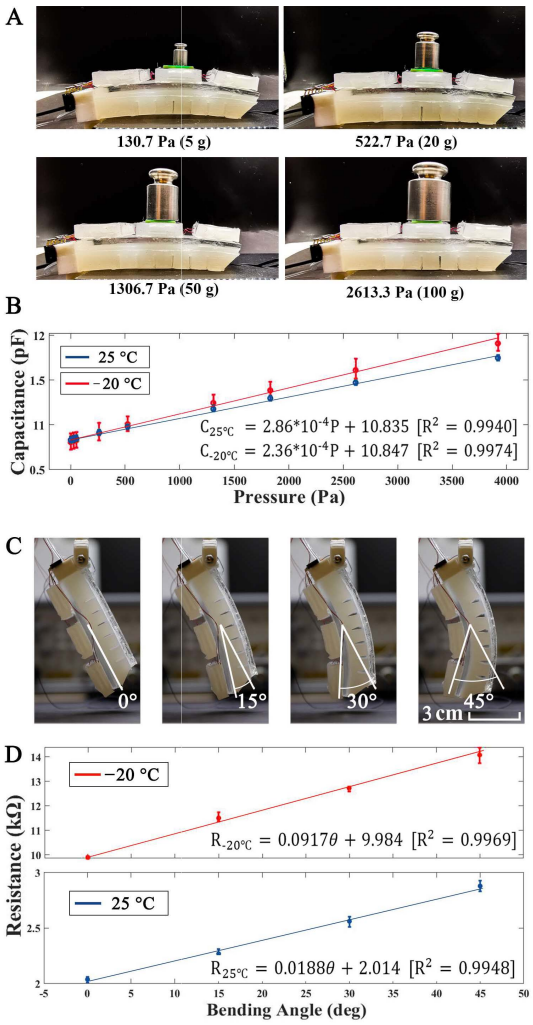

Fig. 4. Calibration of the strain and tactile sensors. (A) Image sequence of a capacitive tactile sensor being calibrated using standard weights. (B) Calibration data of the capacitive tactile sensor output as a function of applied pressure at 25 ° and −20 °C (n = 5). (C) Image sequence of a gripper finger at four bending angles. (D) Calibration data of the sensor resistance output as a function of the finger bending angle at 25 ° and −20 °C (n = 5).

as shown in Fig. 2B. The surface chemical grafting method was used to bond the two hydrogel layers with the EcoFlex layer. The two hydrogel layers were connected to two metal wires of a multiplexer for measuring the capacitance of the sensor. When the soft tactile sensor is compressed upon contact, the thickness of the dielectric layer will decrease, resulting in an increase in the capacitance of the sensor. To achieve high electrical insulation and encapsulation, the entire tri-layer structure was dip-coated with a thin layer of EcoFlex-0050. Additionally, the EcoFlex encapsulation can also enhance the ambient stability of the sensor and make it easy to use. Such tactile sensors can be easily attached to any elastomer-based soft robotic structure using silicone glue.

The capacitive tactile sensor was calibrated using standard weights. As shown in Fig. 4A, a series of standard weights were placed on top of a capacitive tactile sensor for calibration with a thin hardboard between them. The thin hardboard can ensure that the contact area on the capacitive sensor remains the same during calibration. Then the pressure was calculated using the weight and the contact area. Fig. 4B shows two calibration curves of the sensor at 25 °C and −20 °C. It can be observed that the capacitance output increases linearly with the external pressure at both temperatures. In addition, the capacitance output at a certain external pressure only decreases slightly when the environment temperature is changed from 25 °C to −20 °C because of the antifreezing property of the ionic hydrogel. These results are consistent with the previous study [39].

D. Resistive Strain Sensor

The strain sensor material consists of one layer of ionic hydrogel sandwiched between two thin EcoFlex layers, as shown in Fig. 2C. The sensor was cut into a U shape to increase its sensitivity and facilitate wire routing. In comparison with a straight I-shaped sensor, the U-shaped sensor can provide a higher output at the same finger bending angle, and metal wires connected to the ionic hydrogel layer can be routed out from the finger root. Fig. 4C shows an image sequence of a gripper finger bent at different bending angles. The resistance of the U-shaped sensor (Fig. 4D) increases linearly with the bending angle at both room temperature (25 °C) and freezing temperature (−20 °C). The resistance output of the sensor at −20 °C is much higher than that at 25 °C due to the reduced mobility of the ions in the hydrogel.

E. Sensor Integration

To provide information on both deformation and contact, each finger of the soft gripper was equipped with three tactile sensors and one strain sensor. As shown in Fig. 2D, the three tactile sensors are placed on the inner surface of the finger with equal spacing, and the strain sensor is attached to the whole back surface. The tactile sensor can provide feedback regarding contact pressure between the gripper finger and an object, while the strain sensor can provide feedback regarding the finger bending angle. Furthermore, the pressure feedback from the three tactile sensors is spatially distributed along the inner surface of the soft finger, which is suitable for object recognition and force-controlled grasping.

Our sensor integration strategy for the tactile sensors can be further expanded to the integration of a high-density tactile sensor array on the inner surfaces of all three gripper fingers. Based on the current fabrication process, the smallest size of the capacitive force sensor we can achieve is 5 mm × 5 mm. Using such small sensors, it is feasible to implement a 10 × 5 sensor matrix on each finger, which will provide richer tactile information during operation.

III. Object Grasping and Tactile Recognition

A. System Setup

The control system setup of the soft gripper is shown in Fig. 5. A pneumatic pressure source was controlled by an Arduino board (Mega 2560) to independently inflate, hold and deflate the pneumatic networks of three gripper fingers. An LCR meter (E4980A, Agilent) was connected with two

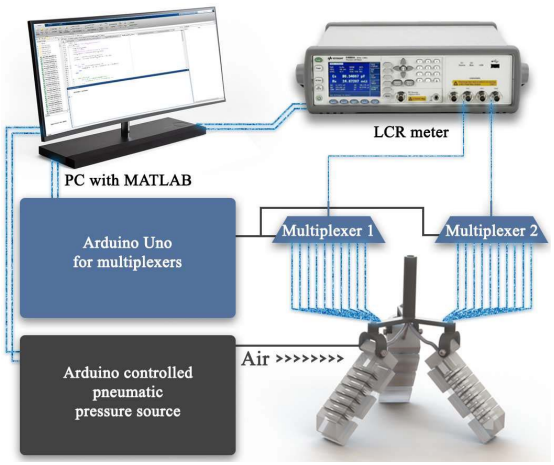

Fig. 5. Schematic of the control system setup for the soft gripper.

high-precision multiplexers (MUX36S16, Taxes Instruments) for capacitance measurements of the nine capacitive tactile sensors. A three-channel Wheatstone circuit was connected to the Arduino board for resistance measurement of the three strain sensors. Both the gripper control and the data acquisition were implemented simultaneously in MATLAB. Moreover, the soft gripper was integrated on a robotic arm (Rotrics DexArm) for grasping objects (Fig. 1).

B. Object Grasping Procedure

In one cycle of object grasping and tactile recognition, the robotic arm first moves the soft robotic gripper to approach the object. Then the open-loop pneumatic pressure source actuates the three fingers to grasp the object for a certain period of time before releasing it. For all the 10 objects grasped in our experiments, an actuation pressure of 6 psi was used to ensure a firm grasp. Throughout the whole process, the strain sensors and tactile sensors continuously collected time-series sensing data for object recognition. All the recognition was performed without lifting the object, which eliminates the possibility that our deep learning model only learns the weight of the object. Fig. 6A illustrates the time-series resistance data collected from the three strain sensors and the capacitance data collected from the nine tactile sensors when an orange was grasped by the soft gripper. As shown in Fig. 6A, when the soft finger was pressurized to grasp the object from the time of 0s to the time of 15s, the resistance of the strain sensors on all three fingers was increased, which means all the fingers were bending simultaneously. The capacitance of the tip and middle tactile sensors on the fingers began to increase when the soft fingers made a contact with the object at about the time of 6s. From the time 15s to 25s, the air pressure of the soft finger was kept, and the soft finger will hold the object, thus the resistance of all the strain sensors and the capacitance of all the tactile sensors remain a constant value. From the time 25s to 32s, the soft finger was depressurized to release the object, and the resistance of the strain sensors and the capacitance of the tip and middle tactile sensors on all three fingers was decreased to zero, which means all the fingers were

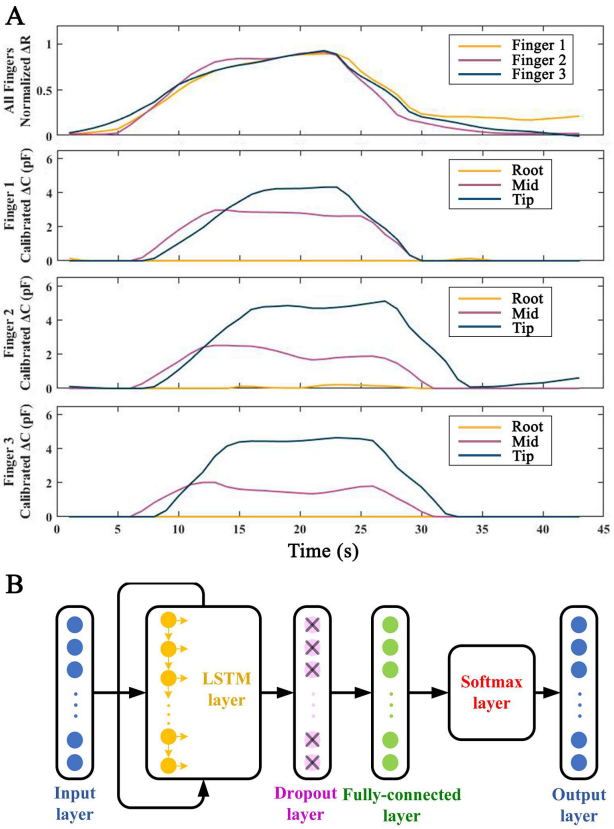

Fig. 6. Learning-based object recognition. (A) Typical time series data of grasping an orange. (B) Schematic of 5-layer LSTM deep learning neural network architecture.

straightened and the object was not in contact with objects. Since the size of the orange is relatively small compared to the size of the soft gripper, the root sensor was not in contact with the object during grasping and thus the capacitance of all the root sensors was kept at 0 all the time. The raw time series data shown in Fig. 6A were directly used for learning-based object recognition in the following part.

C. Learning-Based Object Recognition

To perform object recognition, time-series sensing data of the strain and tactile sensors can provide more information about the grasping process and thus enable the deep learning model to have higher accuracy. Compared with some widely-used neural networks, including CNN and Mask R-CNN, the long short-term memory (LSTM) network, which is a special kind of RNN, is capable of learning long-term dependencies by storing the intermediate state information over extended time intervals. Therefore, a five-layer long short-term memory (LSTM) network was suitable for processing the time series sensor data of the grasping process and was adopted for object recognition experiments. The design, training, validation, and testing of the LSTM network were all implemented through the MATLAB Deep Learning Toolbox. The architecture of the LSTM network is illustrated in Fig. 6B. The input layer contains 12 features that correspond to 12-dimensional time series sensor data gathered from 12 sensors of the soft gripper. The LSTM layer is designed to have 128 hidden units,

followed by a dropout layer and a fully connected layer. The dropout layer rate was set as 0.2, and then a transfer function SoftMax was used. Finally, a total of 11 outputs are provided by the output layer, which corresponds to the 11 labels for 10 objects as well as an empty grasp.

D. Closed-Loop Force Control

The capacitive tactile feedback of the gripper provides contact force information when the soft gripper grasps an object, which can also be used for grasping force control. To demonstrate how the capacitive tactile sensors are used for delicate grasping, a conventional proportional-integral-derivative (PID) force controller was designed to allow the soft gripper to apply an accurate grasping force (especially useful for grasping fragile objects). Note the relationship between the contact force and the sensor output depends on the contact area. Therefore, we directly regulated the capacitance output of a tactile sensor using the PID controller. Although each gripper finger integrates three tactile sensors, we only controlled capacitance outputs of the three tactile sensors at the fingertips as the contact feedback; this allowed us to regulate the grasping forces at the three fingertips. The structure of the PID force controller is shown in Fig. 7A. The input of the PID force controller is the capacitance error of the tactile sensor, which is the difference between the expected capacitance and the measured feedback capacitance. Accordingly, the PID controller regulates the voltage of the proportional control valve through an Arduino board (Mega 2560) and an L298N motor driver to adjust the flow rate and thus the pressure for gripper finger inflation.

To evaluate the performance of the PID force controller, we first tuned the three PID parameters through force-controlled grasping of an Ecoflex bottle (450 g) and measured the closed-loop controlled capacitance output of the sensor. We first tuned the parameter K_I and K_D and set them as $K_I = 0.005$, and $K_D = 0.01$. Then the tuning of the parameter K_P and the corresponding capacitive response are shown in Fig. 7B. We finally chose the parameters $K_P = 0.3$, $K_I = 0.005$, and $K_D = 0.01$, which provide a rising time of 11.6 s and a steady-state error of 3.44%. We also showed the tracking of step-wise increases of the sensor output capacitance, as shown in Fig. 7C. With the PID force controller, the soft gripper can realize new functions such as force-controlled grasping of fragile or highly deformable objects as well as object slip detection and compensation. These functions will be demonstrated in Section IV.

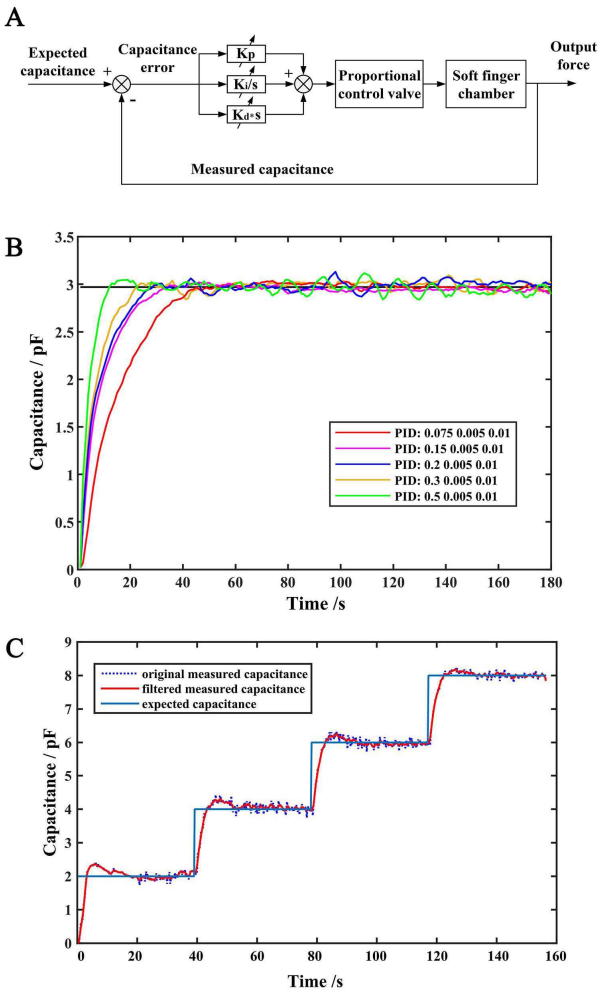

Fig. 7. Design and characterization of the closed-loop PID force controller for the sensory soft gripper. (A) Schematic of closed-loop PID force controller. (B) Tuning of parameter K_P and the corresponding capacitive response of the PID force controller during grasping of an EcoFlex bottle (450 g). (C) Step response of the PID force controller.

IV. Experimental Results

In order to evaluate the performance of the sensory soft gripper, object grasping and recognition experiments were first conducted. Ten typical objects of different shapes, sizes, and materials were grasped at room temperature (25 °C), and then object recognition was performed based on the time-series sensor data and the deep learning method. A video of grasping demonstration and learning-based recognition can be found in Video S2, Supplementary Videos. Next, we also conducted grasping and object recognition of five objects at a freezing temperature (−20 °C) to demonstrate the performance of the gripper in cold environments. Finally, a closed-loop force control experiment was conducted and a slip detection and compensation strategy was tested.

A. Learning-Based Object Recognition

In the object recognition experiment, 10 typical objects were grasped by the soft gripper at room temperature (25 °C), as shown in Fig. 8A. The objects were chosen to have different shapes, sizes, and materials. There are still some objects that are similar in shape or size (e.g., lemon and orange) in order to verify the effectiveness of the model. During the grasping of an object, the strain and tactile sensors can provide information about the deformation of the soft fingers, as well as the contact pressure and locations between the object and the fingers. Then the information was used by the deep learning model for object recognition. Since it is a dynamic process for the soft gripper to grasp an object, we collected time-series data from the 12 sensors to obtain information about the entire

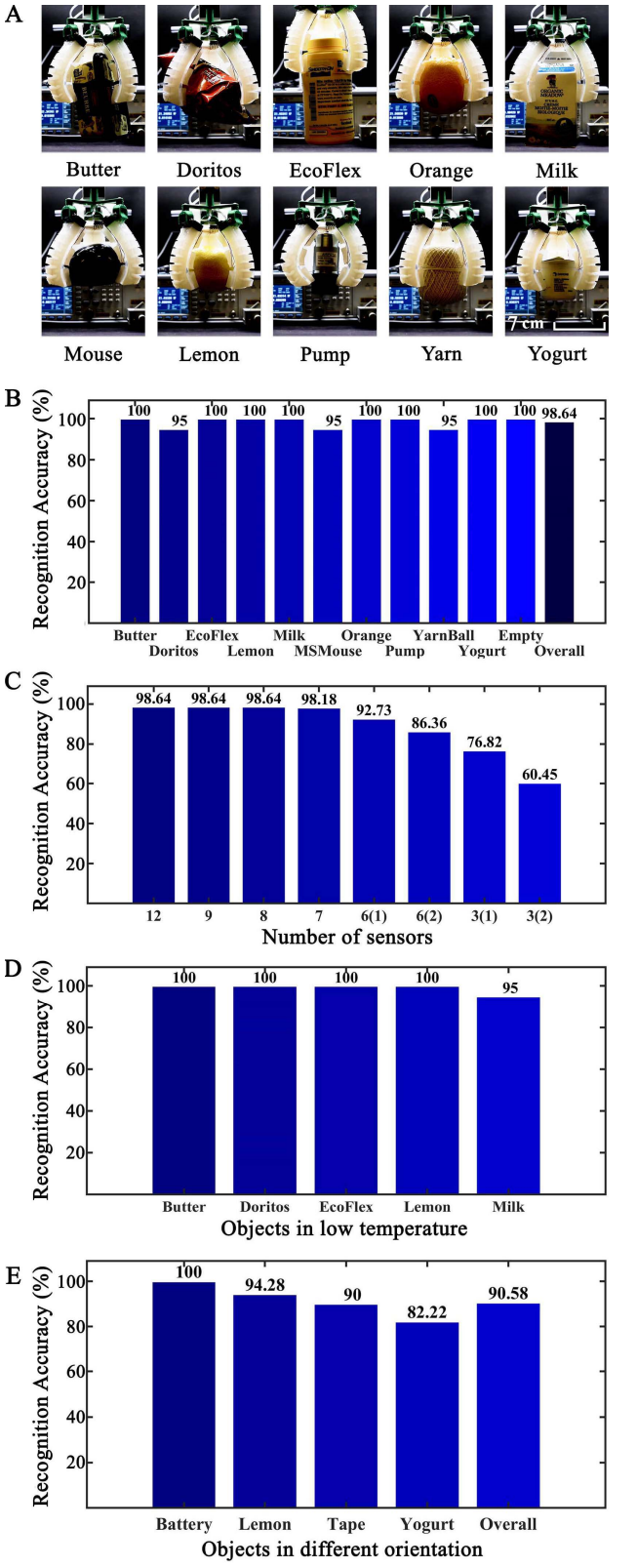

Fig. 8. Learning-based object recognition experiments. (A) Stable grasp of 10 objects for object recognition. (B) The object recognition accuracy of 10 objects and an empty grasp. (C) Overall object recognition accuracy using data from different numbers of sensors. (D) The object recognition accuracy of five objects at freezing temperature (−20 °C). (E) The object recognition accuracy of four objects of different orientations.

process. The time-series data collection process is described in Section III-B. Each object was grasped 20 times to establish a time-series data set for object recognition. For the 10 typical objects, we will have 200 time-series data in total. To take advantage of the data, the K-fold cross-validation method was applied in the training. During each grasp, the object remained approximately in the same position and orientation, and the soft robotic gripper approached the object from above and grasped it at a fixed angle. The stable grasping of each object is shown in Fig. 8A.

The LSTM network was trained and evaluated on five-fold cross validation due to the limitation of obtaining large data sets from the soft gripper. The original data set was split into five folds randomly. For each round of cross validation, four folds were used to train the LSTM network, and the last fold was used as the validation and test set. After all rounds of five-fold cross validation finished, the average object recognition accuracy was shown in Fig. 8B-E. The network was trained using the Adam Optimizer, and L2 regularization was used to avoid over-fitting. The total training process for the 10-object recognition took about 1.5 hours. The recognition accuracy was averaged over the five rounds of cross validation. Fig. 8B shows the object recognition accuracy of the 10 objects and an empty grasp. The results show that the object recognition based on the sensor data and the learning method has a high accuracy: the overall recognition accuracy for all objects is 98.64%. Seven objects can be recognized with 100% accuracy. Only three objects (Doritos bag, milk carton, and pump) were recognized with errors, and their average recognition accuracy is 95%. The lemon and orange have similar sizes and shapes, but the LSTM learning method is capable distinguish them successfully. These results demonstrate that the sensory soft gripper can recognize the 10 objects accurately at room temperature using the sensor data and the LSTM network.

For object recognition with the LSTM network, we found that using data from all 12 sensors provides the same accuracy as using data from only the nine tactile sensors, as shown in Fig. 8C. In this figure, the x-axis indicates the number of sensors, where 12 means object recognition accuracy using data from three bend sensors and 9 force sensors; 9 means using data of all tip, middle, and root force sensors on 3 fingers; 8 means using data of 8 sensors; 6(1) means using data of middle and root sensors on 3 fingers; 6(2) means using data of all tip, middle and root sensors on two fingers; 3(1) means using data of three tip sensors; and 3(2) means using data of three root sensors. It is obvious in Fig. 8C that the three strain sensors on the finger back surface do not significantly contribute to the object recognition based on our small set of objects; however, they are necessary for other functions of the soft gripper, for example, measuring the bending angle of each finger and performing closed-loop control of the finger motion. As shown in Fig. 8C, reducing the number of tactile sensors to 7 tactile sensors will not affect the recognition accuracy, but if we continue to reduce the number of sensors, the recognition accuracy will decrease sharply. Also, reducing the number of sensors can simplify the computational cost of the training

algorithm. For our future work on object recognition using a large set of objects, the data from the finger strain sensors and the arrangement of more than three tactile sensors on each finger may be necessary.

B. Object Recognition at Freezing Temperature

To demonstrate the antifreezing property of the hydrogel-based sensors, object grasping and recognition experiments were conducted inside a chest freezer at freezing temperatures (−20 °C). Five objects were selected for this experiment from the original dataset of 10 objects. Each object was grasped 20 times at −20 °C and the time-series data of all the sensors were collected during grasping to obtain a new dataset for the LSTM network. Five-fold cross validation was also used to evaluate the network. Fig. 8D shows the results of object recognition accuracy at −20 °C for the five objects and the empty grasp. The overall recognition accuracy is 99.0%. The results indicate that the hydrogel-based sensors on the soft robotic gripper are capable of providing reliable data for object recognition at both room and freezing temperatures.

C. Recognition of Objects With Different Orientations

We also demonstrated the gripper's capability of grasping and recognizing objects with different orientations. We collected the time series sensor data of grasping a set of four objects with different orientations. In this four-object data set, lemon and yogurt were chosen from the original 10-object set for recognition, while battery and tape were new objects. To make the experiments manageable, we choose four different orientations of each object for training data collection. At each orientation, objects were grasped 20 times to form a time series data set for learning-based object recognition. We used the same LSTM network as in previous experiments. The five-fold cross validation method was used to evaluate the object recognition accuracy. Fig. 8E shows the recognition accuracy values for the four objects with different orientations. The overall recognition accuracy of all four objects is 90.58%. These results confirm that it is feasible to use the sensory gripper to accurately recognize objects even though they are at different orientations.

D. Force-Controlled Grasping of Fragile or Highly Deformable Objects

Although the soft gripper can successfully grasp many objects without force control thanks to its high compliance, there are still certain fragile or highly deformable objects that require gentle grasping and may be damaged by the soft gripper (if the grasping force is not carefully regulated). The closed-loop PID force controller detailed in Section III-D can be used in such a case to accurately control the grasping force applied to the object. Here, we demonstrated a case study on the force-controlled grasping of a plastic weighing boat commonly used for chemical mass measurement (Video S3, Supplementary Videos). We found that when the soft gripper grasps the weighing boat without force control, it was experimentally challenging to regulate the inflation flow

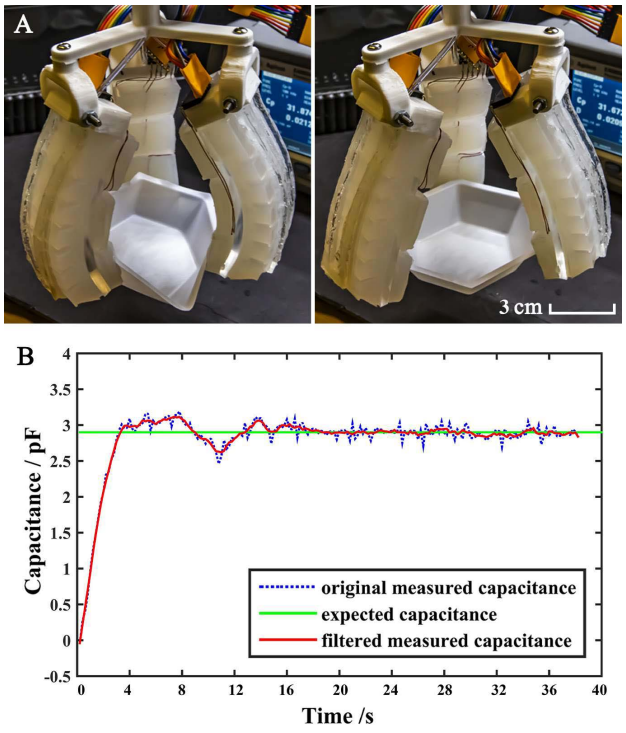

Fig. 9. Comparison of the open-loop pinch grasp and the closed-loop pinch grasp (A) Grasps of a weighing boat using the open-loop controller and the closed-loop PID force controller respectively. (B) Capacitance response of the closed-loop PID force controller when the soft gripper pinches a weighing boat.

rate of the gripper fingers to ensure secured grasping and in the meanwhile avoid large deformation (and thus structural instability) of the weighing boat (Fig. 9A). When the PID force controller was used to control the contact force between the plastic weighing boat and the tip tactile sensors, secured grasping with a gentle contact force was readily achieved (Fig. 9B). Fig. 9B shows the closed-loop controlled output of the tip tactile sensor when the soft gripper pinched a weighing boat of 1.64 g.

E. Force-Controlled Slip Detection and Compensation

With the closed-loop PID force controller, the soft gripper can grasp objects with accurately controlled grasping force. Nevertheless, when the gripper grasps a heavy object from a surface and then lifts it, a slip may occur. Based on the contact force feedback and the PID force controller, we proposed a real-time strategy to detect potential slips during heavy object lifting and conduct online slip compensation accordingly. In most cases, an object slipping in the gripper will constantly contact the tip tactile sensors before it completely slips out of the gripper. Therefore, our strategy is to monitor the force feedback from the middle and tip tactile sensors for slip detection and adjust the grasping force level of the tip tactile sensors accordingly based on the PID force control. A video showing the slip detection and compensation can be found in Video S3, Supplementary Videos.

When grasping objects of different shapes and sizes, the soft gripper operates in one of two grasp modes: i) tip pinch: only

Algorithm 1 Algorithm for the Slip Detection and Compensation Strategy

Require: Capacitance reading of the tip tactile sensors $C_{t,i}$ and middle tactile sensors $C_{m,i}$ on the three soft fingers ($i = 1, 2, 3$)

procedure SLIPDETECTIONCOMPENSATION($C_{t,i}$, $C_{m,i}$)
  Pressurize the soft gripper to grasp the object
  Define two grasp modes based on the middle sensor reading $C_{m,i}$ or root sensor reading $C_{r,i}$
  Grasp mode 1: Tip Pinch ($C_{m,i}$ =0 and $C_{r,i}$ = 0)
  if $C_{t,i}$ decrease sharply to 0 **then**
    Slip detected, object already fell from the gripper
    Depressurize the soft gripper
    Grasp the object again with larger air pressure
  else
    Slip not detected, the object is grasped stably by the gripper
  end if
  Grasp mode 2: Wrap Grasp ($C_{m,i} \neq 0$ or $C_{r,i} \neq 0$)
  if $C_{m,i}$ (or $C_{r,i}$) decrease sharply to 0 **then**
    Slip detected, the object is falling from the gripper
    Increase the air pressure of the soft gripper for compensation
  else
    Slip not detected, the object is grasped stably by the gripper
  end if
end procedure

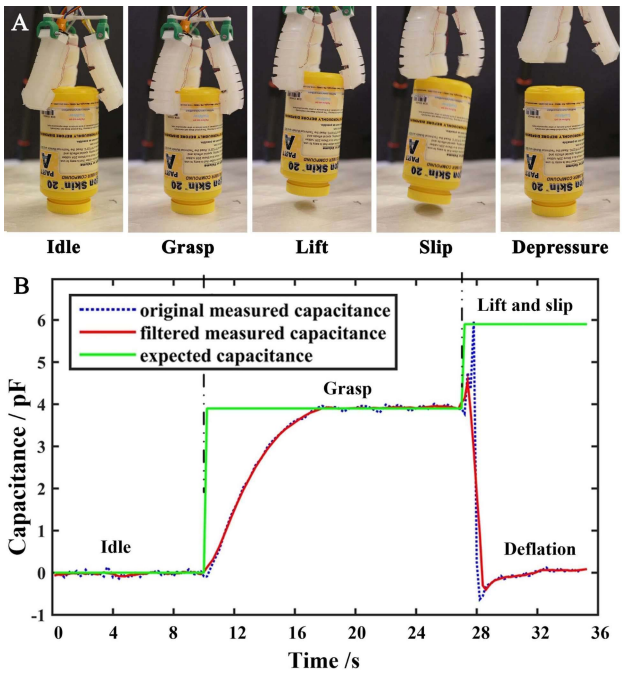

Fig. 10. Slip detection and compensation strategy for tip pinch. (A) pinch grasp and lift of an eco-flex bottle with slip detection and compensation. (B) the corresponding capacitive responses of a tip sensor for slip detection and compensation strategy.

the tip tactile sensors contact the object; and ii) wrap grasp: at least the middle and tip tactile sensors contact the object. The slip detection and compensation strategy works differently for those two grasp modes, as shown in Algorithm 1. In the tip pinch mode, slip can be detected when the capacitance output of a tip tactile sensor decreases sharply to near zero. However, in this case, the drop of the tip sensor output is too rapid to re-adjust the tip grasping force to re-secure the grasp. Thus, the compensation strategy is to adjust the expected capacitance of the PID controller to zero so that the gripper is depressurized to prevent over-inflation and damage. Then, the soft gripper can grasp the object again with increased reference input for the PID force controller. As shown in Fig. 10A, the gripper was trying to pinch and lift a heavy EcoFlex bottle (450 g), and the bottle dropped during the lifting process. Fig. 10B shows the capacitance output data of the PID controller on one tip tactile sensor, which reveals the contact force change in the stages of slip detection and compensation.

For the wrap grasp mode, the gripper fingers have a large initial contact area with an object to force a wrap grasp, which makes at least the middle and tip tactile sensors (in some cases also the root and tip sensors) in contact with the object. In such a case, slip can be detected by monitoring any rapid decrease of the middle sensor output. Because of the large contact area of the wrap grasp, once the slip is detected, the PID controller will usually have sufficient time to increase the grasping force level at the fingertips to prevent the object from completely dropping out of the gripper. When the capacitance output of a middle or root tactile sensor decreases sharply to near zero during the lifting process, the slip is detected and the expected capacitance of the PID force controller is then increased by a certain level for compensation to enable larger air pressure of the soft gripper and thus a firmer grasp. The EcoFlex bottle (450 g) and the yogurt container were chosen from the ten objects of object recognition set to demonstrate the slip detection and compensation strategy for wrap grasp. Fig. 11A shows the process of slip detection and compensation when the soft gripper wraps and lifts the EcoFlex bottle. Figs. 11B and 11C show the capacitance change of the middle tactile sensor and the corresponding capacitance output of the PID force controller on the tip sensor, respectively.

In the PID force control results (Fig. 10B, 11B and 11C) of both tip pinch and wrap grasp modes, it can be noticed that when the soft gripper started to grasp a heavy object (sitting on a surface), an expected capacitance (thus force) output of the tip sensor was set for the PID force controller to enable the initial grasping. When the soft gripper began to lift the object, the lifting of the heavy object introduced a shear force to the tip tactile sensors and thus the measured sensor output increased and became larger than the originally set capacitance level. Thus during the lifting of heavy objects, we need to online tuning the expected capacitance output of the PID force controller by an increased step to ensure that the PID force controller will not decrease the air pressure of the soft gripper sharply when lifting. After many tests about the different increased steps of the expected capacitance, we set the increased step as 2pF for our soft gripper lifting

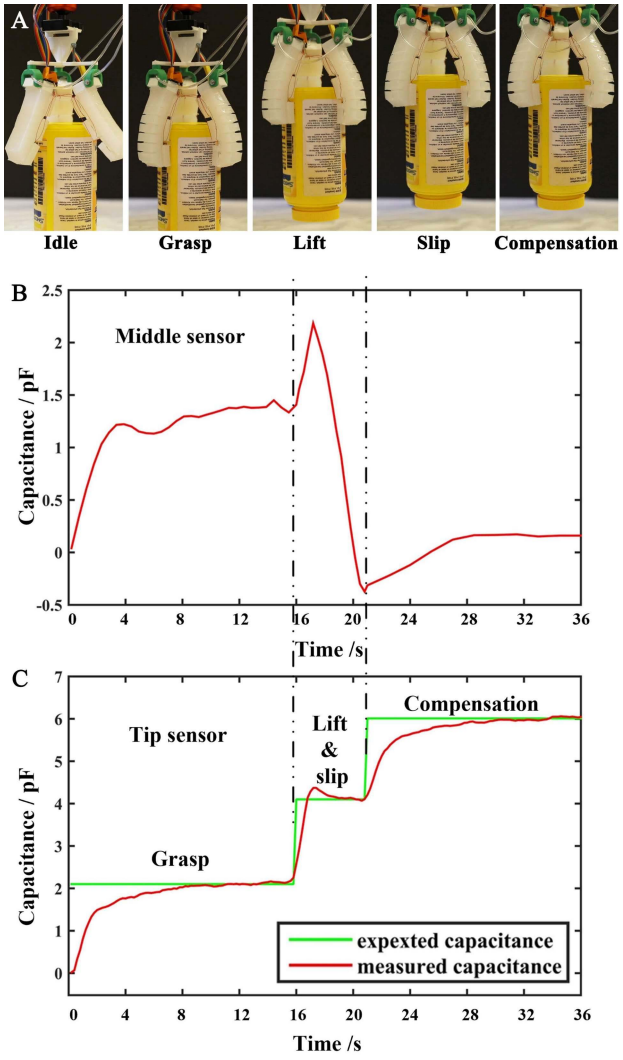

Fig. 11. Slip detection and compensation strategy for wrap grasp. (A) wrap grasp and lift an Ecoflex bottle with slip detection and compensation. (B) the corresponding capacitive response of a middle sensor. (C) the corresponding capacitive response of a tip sensor for slip detection and compensation strategy.

heavy objects. Such value will ensure that the air pressure of the soft gripper will not change too much and the soft gripper is still able to grasp the heavy objects with enough force after lifting.

V. Conclusion

A three-finger soft gripper with ionic hydrogel-based strain and tactile sensors was presented in this paper. Stretchable, ambient-stable, and antifreezing ionic hydrogel was used to fabricate the strain and tactile sensors, which matched the mechanical properties of the elastomer-based soft gripper. The sensors can be used to measure the bending angle of the soft finger during object grasping as well as the contact pressure between the finger and an object. The antifreezing feature of the hydrogel-based sensors allowed them to reliably operate at freezing temperatures. An LSTM deep-learning network was employed to assimilate the sensor feedback data for object recognition, and achieved recognition accuracy values of i) 98.64% for 10 objects at room temperature (25 °C); ii) 99.0% for five objects at a freezing temperature (−20 °C); and iii) 90.58% for four objects with different orientations. We also realized closed-loop PID control of the tip grasping force (based on tip tactile sensor feedback), and proposed and validated a slip detection and compensation strategy to effectively handle possible object slippage during lifting. These results demonstrate the ability of our sensory soft gripper for accurate object recognition, force-controlled grasping, and force-feedback-based slip detection and compensation.

Our three-finger soft sensory gripper still has some limitations that are needed to be improved. Firstly, the maximal cylindrical object that can be grasped by the soft gripper has a diameter of 120 mm because the distance between the soft fingers and the tilted angle of each finger cannot be adjusted to adapt to objects of different sizes and shapes. In the future, we can improve the design of the soft gripper to endow it with new capabilities to adjust the configuration of all the fingers to grasp objects of a large range of sizes. Secondly, the hydrogel sensor attached to the fingertip can only detect the total normal force applied on the whole sensor surface, instead of the lateral force or the exact position of the applied force. In our future work, it is possible to further expand our capacitive force sensor configuration to a higher-density tactile sensor array, which will enhance the spatial resolution of tactile sensing and enable the detection of lateral force and the applied position of the normal force. Thirdly, our LSTM deep learning model for object recognition was only implemented on a small set of objects because collecting tactile sensing data of a large number of objects is time-consuming. We think the deep learning method based on the sensor data has the potential to recognize a large set of objects if we establish a large sensor data set to train it. This will be our immediate future work on this project. Finally, the slip compensation method can only be used for objects that are in contact with middle or root sensors so that it has enough time to detect slip and control the gripper to apply more force. However, if we grasp an object with only the fingertips, the slip can only be detected after the object slips from the gripper. This can be solved by using a high-resolution sensor array that can detect shear force on the fingertip, which will be another direction related to this work that is worth further investigation.

References

[1] Q. Liu, X. Gu, N. Tan, and H. Ren, "Soft robotic gripper driven by flexible shafts for simultaneous grasping and in-hand cap manipulation," *IEEE Trans. Autom. Sci. Eng.*, vol. 18, no. 3, pp. 1134–1143, Jul. 2021.

[2] D. Rus and M. T. Tolley, "Design, fabrication and control of soft robots," *Nature*, vol. 521, no. 7553, pp. 467–475, May 2015.

[3] B. S. Homberg, R. K. Katzschmann, M. R. Dogar, and D. Rus, "Robust proprioceptive grasping with a soft robot hand," *Auto. Robots*, vol. 43, no. 3, pp. 681–696, Mar. 2019.

[4] N. Tan, X. Gu, and H. Ren, "Pose characterization and analysis of soft continuum robots with modeling uncertainties based on interval arithmetic," *IEEE Trans. Autom. Sci. Eng.*, vol. 16, no. 2, pp. 570–584, Apr. 2019.

[5] J. Zimmer, T. Hellebrekers, T. Asfour, C. Majidi, and O. Kroemer, "Predicting grasp success with a soft sensing skin and shape-memory actuated gripper," in *Proc. IEEE/RSJ Int. Conf. Intell. Robots Syst. (IROS)*, Nov. 2019, pp. 7120–7127.

[6] S. Li et al., "A vacuum-driven origami 'magic-ball' soft gripper," in *Proc. Int. Conf. Robot. Autom. (ICRA)*, May 2019, pp. 7401–7408.

[7] M. Liarokapis and A. M. Dollar, "Combining analytical modeling and learning to simplify dexterous manipulation with adaptive robot hands," *IEEE Trans. Autom. Sci. Eng.*, vol. 16, no. 3, pp. 1361–1372, Jul. 2019.

[8] Y. Wang and Q. Xu, "Design and testing of a soft parallel robot based on pneumatic artificial muscles for wrist rehabilitation," *Sci. Rep.*, vol. 11, no. 1, pp. 1–11, Jan. 2021.

[9] Q. Yu, W. Shang, Z. Zhao, S. Cong, and Z. Li, "Robotic grasping of unknown objects using novel multilevel convolutional neural networks: From parallel gripper to dexterous hand," *IEEE Trans. Autom. Sci. Eng.*, vol. 18, no. 4, pp. 1730–1741, Oct. 2021.

[10] J. Shi and G. S. Koonjul, "Real-time grasping planning for robotic bin-picking and kitting applications," *IEEE Trans. Autom. Sci. Eng.*, vol. 14, no. 2, pp. 809–819, Apr. 2017.

[11] D. Trivedi, C. D. Rahn, W. M. Kier, and I. D. Walker, "Soft robotics: Biological inspiration, state of the art, and future research," *Appl. Bionics Biomech.*, vol. 5, no. 3, pp. 99–117, 2008.

[12] T. G. Thuruthel, B. Shih, C. Laschi, and M. T. Tolley, "Soft robot perception using embedded soft sensors and recurrent neural networks," *Sci. Robot.*, vol. 4, no. 26, Jan. 2019, Art. no. eaav1488.

[13] R. L. Truby, C. D. Santina, and D. Rus, "Distributed proprioception of 3D configuration in soft, sensorized robots via deep learning," *IEEE Robot. Autom. Lett.*, vol. 5, no. 2, pp. 3299–3306, Apr. 2020.

[14] Y.-L. Park, B.-R. Chen, and R. J. Wood, "Design and fabrication of soft artificial skin using embedded microchannels and liquid conductors," *IEEE Sensors J.*, vol. 12, no. 8, pp. 2711–2718, Aug. 2012.

[15] C. Majidi, Y.-L. Park, R. Kramer, P. Bérard, and R. J. Wood, "Hyperelastic pressure sensing with a liquid-embedded elastomer," *J. Micromech. Microeng.*, vol. 20, no. 12, p. 125029, 2010.

[16] D. M. Vogt, Y.-L. Park, and R. J. Wood, "Design and characterization of a soft multi-axis force sensor using embedded microfluidic channels," *IEEE Sensors J.*, vol. 13, no. 10, pp. 4056–4064, Oct. 2013.

[17] Y.-L. Park, S. C. Ryu, R. J. Black, K. K. Chau, B. Moslehi, and M. R. Cutkosky, "Exoskeletal force-sensing end-effectors with embedded optical fiber-Bragg-grating sensors," *IEEE Trans. Robot.*, vol. 25, no. 6, pp. 1319–1331, Dec. 2009.

[18] C. To, T. L. Hellebrekers, and Y.-L. Park, "Highly stretchable optical sensors for pressure, strain, and curvature measurement," in *Proc. IEEE/RSJ Int. Conf. Intell. Robots Syst. (IROS)*, Sep. 2015, pp. 5898–5903.

[19] H. Zhao, K. O'Brien, S. Li, and R. F. Shepherd, "Optoelectronically innervated soft prosthetic hand via stretchable optical waveguides," *Sci. Robot.*, vol. 1, no. 1, Dec. 2016, Art. no. eaai7529.

[20] Y. She, S. Q. Liu, P. Yu, and E. Adelson, "Exoskeleton-covered soft finger with vision-based proprioception and tactile sensing," in *Proc. IEEE Int. Conf. Robot. Autom. (ICRA)*, May 2020, pp. 10075–10081.

[21] J. Hughes, S. Li, and D. Rus, "Sensorization of a continuum body gripper for high force and delicate object grasping," in *Proc. IEEE Int. Conf. Robot. Autom. (ICRA)*, May 2020, pp. 6913–6919.

[22] B. S. Homberg, R. K. Katzschmann, M. R. Dogar, and D. Rus, "Haptic identification of objects using a modular soft robotic gripper," in *Proc. IEEE/RSJ Int. Conf. Intell. Robots Syst. (IROS)*, Sep. 2015, pp. 1698–1705.

[23] Y. She, C. Li, J. Cleary, and H.-J. Su, "Design and fabrication of a soft robotic hand with embedded actuators and sensors," *J. Mech. Robot.*, vol. 7, no. 2, pp. 1–9, May 2015.

[24] C. M. Boutry et al., "A hierarchically patterned, bioinspired e-skin able to detect the direction of applied pressure for robotics," *Sci. Robot.*, vol. 3, no. 24, Nov. 2018, Art. no. eaau6914.

[25] S. Y. Kim et al., "Sustainable manufacturing of sensors onto soft systems using self-coagulating conductive pickering emulsions," *Sci. Robot.*, vol. 5, no. 39, 2020, Art. no. eaay3604.

[26] A. Frutiger et al., "Capacitive soft strain sensors via multicore–shell fiber printing," *Adv. Mater.*, vol. 27, no. 15, pp. 2440–2446, 2015.

[27] R. L. Truby et al., "Soft somatosensitive actuators via embedded 3D printing," *Adv. Mater.*, vol. 30, no. 15, Apr. 2018, Art. no. 1706383.

[28] G. Gu et al., "Integrated soft ionotronic skin with stretchable and transparent hydrogel-elastomer ionic sensors for hand-motion monitoring," *Soft Robot.*, vol. 6, no. 3, pp. 368–376, 2019.

[29] B. Ying, Q. Wu, J. Li, and X. Liu, "An ambient-stable and stretchable ionic skin with multimodal sensation," *Mater. Horizons*, vol. 7, no. 2, pp. 477–488, 2020.

[30] B. Ying and X. Liu, "Skin-like hydrogel devices for wearable sensing, soft robotics and beyond," *iScience*, vol. 24, no. 11, Nov. 2021, Art. no. 103174.

[31] S. Cheng, Y. S. Narang, C. Yang, Z. Suo, and R. D. Howe, "Stick-on large-strain sensors for soft robots," *Adv. Mater. Interfaces*, vol. 6, no. 20, Oct. 2019, Art. no. 1900985.

[32] B. Ying, R. Z. Chen, R. Zuo, J. Li, and X. Liu, "An anti-freezing, ambient-stable and highly stretchable ionic skin with strong surface adhesion for wearable sensing and soft robotics," *Adv. Funct. Mater.*, vol. 31, no. 42, Oct. 2021, Art. no. 2104665.

[33] R. Zuo, Z. Zhou, B. Ying, and X. Liu, "A soft robotic gripper with anti-freezing ionic hydrogel-based sensors for learning-based object recognition," in *Proc. IEEE Int. Conf. Robot. Autom. (ICRA)*, May 2021, pp. 12164–12169.

[34] F. Ilievski, A. D. Mazzeo, R. F. Shepherd, X. Chen, and G. M. Whitesides, "Soft robotics for chemists," *Angew. Chem.*, vol. 123, no. 8, pp. 1930–1935, Feb. 2011.

[35] B. Mosadegh et al., "Pneumatic networks for soft robotics that actuate rapidly," *Adv. Funct. Mater.*, vol. 24, no. 15, pp. 2163–2170, Apr. 2014.

[36] A. D. Marchese, R. K. Katzschmann, and R. Daniela, "A recipe for soft fluidic elastomer robots," *Soft Robot.*, vol. 2, no. 1, pp. 7–25, 2015.

[37] J.-Y. Sun et al., "Highly stretchable and tough hydrogels," *Nature*, vol. 489, no. 7414, pp. 133–136, Sep. 2012.

[38] H. Yuk, T. Zhang, G. A. Parada, X. Liu, and X. Zhao, "Skin-inspired hydrogel–elastomer hybrids with robust interfaces and functional microstructures," *Nature Commun.*, vol. 7, no. 1, pp. 1–11, Nov. 2016.

[39] Z. Lei and P. Wu, "A supramolecular biomimetic skin combining a wide spectrum of mechanical properties and multiple sensory capabilities," *Nature Commun.*, vol. 9, no. 1, pp. 1–7, Dec. 2018.